Synthesis and Characterization of Sulfur-Bridged Binuclear β-Diketonatoruthenium Complexes and a Monomeric Ruthenium Complex. Crystal and Molecular Structures of Racemic and Meso Isomers of [Ru(acac)$_2$(μ-topd-*O,S,O′*)Ru(acac)$_2$] (acac = Acetylacetonato and topd = 3-Thioxo-2,4-pentanedione)

Takeshi Hashimoto, Akira Endo, Noriharu Nagao, Gen P. Satô, Karuppannan Natarajan,† and Kunio Shimizu*

Department of Chemistry, Faculty of Science and Technology, Sophia University, 7-1 Kioicho, Chiyoda-ku, Tokyo 102, Japan

Received September 30, 1997

A new mode of binding of a β-diketone has been established. Two oxygen atoms and a sulfur atom at the γ-position of the β-diketone bind to two ruthenium atoms with the sulfur forming the bridge. A mononuclear complex has also been isolated in which the β-diketone binds through O and S atoms. The syntheses of mononuclear complex [Ru(acac)$_2$(topd-*O,S*)] (**1**) and binuclear complexes [{Ru(acac)$_2$}$_2$(μ-topd-*O,S,O′*)] (**2**, racemic form), [{Ru(acac)$_2$}$_2$(μ-topd-*O,S,O′*)] (**2′**, meso form), [{Ru(phpa)$_2$}$_2$(μ-topd-*O,S,O′*)] (**3**, racemic form), and [{Ru(phpa)$_2$}$_2$(μ-topd-*O,S,O′*)] (**3′**, meso form) have been described. The crystal and molecular structures of **2** and **2′** have been solved by single-crystal X-ray diffraction studies. Crystal data for **2** ($Ru_2C_{25}H_{34}O_{10}S$): space group $P2_1/n$, $a = 11.388(3)$ Å, $b = 23.390(3)$ Å, $c = 11.978(3)$ Å, $\beta = 93.06(2)°$, $Z = 4$, $R = 0.056$, $R_w = 0.042$. Crystal data for **2′** ($Ru_2C_{25}H_{34}O_{10}S$): space group $P2_1/n$, $a = 16.281(3)$ Å, $b = 21.195(2)$ Å, $c = 21.465(3)$ Å, $\beta = 105.75(1)°$, $Z = 4$, $R = 0.049$, $R_w = 0.042$. The ^{13}C NMR spectra indicate the difference between the mononuclear (**1**) and the binuclear complex (**2′**) in their topd-*C*S signals for the presence of two types of bonding modes for the topd ligand. There is no difference in the electronic spectra of the meso and racemic isomers of the binuclear complexes. The X-ray photoelectron spectrum (XPS) of **1** resembles that of Ru^{III} whereas the spectra of all of the binuclear complexes indicate the presence of both Ru^{III} and Ru^{II}. Cyclic voltammetric studies also corroborate the findings of XPS that the monomeric complex **1** contains Ru^{III} and all of the binuclear complexes have in them both Ru^{III} and Ru^{II}. The electronic structures of the complexes have been discussed on the bases of photoelectron spectra, electronic spectra, and magnetic measurements and electrochemistry.

Introduction

A wide variety of substitution at the γ-position of a β-diketonato chelate ring has been described.[1] Introduction of an ethynyl group at a γ-position of tris(β-diketonato)ruthenium(III) was reported by us earlier.[2,3] However, no such synthesis has been described to introduce a sulfur atom at the γ-position. In this line, we were successful in obtaining a dimeric ruthenium(III) complex containing sulfur-substituted bridging β-diketonate rings.[4] Such sulfur-containing bridging ligands as well as a disulfide between two metal centers are better probes to study the behavior of mixed-valent oxidation states of Ru^{II}/Ru^{III} and Ru^{III}/Ru^{IV}.[5] To introduce directly the sulfur-containing bridging β-diketone rings between two ruthenium metal centers, we carried out the reactions of 3,3′-dithiobis(2,4-pentanedione) (H_2dtba) with [{Ru(β-dik)$_2$(CH$_3$CN)$_2$] (β-dik = 2,4-pentanedionato (acac) or 2,2,6,6,-tetramethylheptanedionato (phpa)). Surprisingly, however, quite unexpected sulfur-bridged binuclear complexes [{Ru(β-dik)$_2$)}$_2$(topd-*O,S,O′*)] and a mononuclear complex [Ru(β-dik)$_2$)(topd-*O,S*)] have been obtained. β-Diketones and related compounds exhibit a number of types of bonding modes,[1] but no tridentate behavior has been shown by any β-diketone in which the γ-position is substituted by a potential donor atom or group. Moreover, to our knowledge, no β-diketone is known to bind to two different metal atoms through the two oxygen atoms with a bridge being formed by a donor atom at the γ-carbon. The racemic and meso isomers of [Ru(β-dik)$_2$(μ-topd-*O,S,O′*)Ru(β-dik)$_2$] are the first examples to show this type of binding of a β-diketone. We report here the synthesis, spectroscopic properties, and voltammetric behavior of the mononuclear and binuclear complexes and the crystal and molecular structures of the binuclear complexes. Though a similar type of mononuclear complex of platinum(II), [Pt(topd-*O,S*)(PMe$_2$Ph)$_2$], has been obtained from [PtCl(PMe$_2$Ph)$_3$]PF$_6$ and H_2dtba, no dimeric species has been isolated.[6]

† Present address: Department of Chemistry, Bharathiar University, Coimbatore, 641046, India.

(1) Mehrotra, R. C.; Bohra, R.; Gaur, D. P. *Metal β-Diketonates and Allied Derivatives*; Academic Press: London, 1978.
(2) Kasahara, Y.; Hoshino, Y.; Kajitani, M.; Shimizu, K.; Satô, G. P. *Organometallics* **1992**, *11*, 1968.
(3) Endo, A.; Kajitani, M.; Mukaida, M.; Shimizu, K.; Satô, G. P. *Inorg. Chim. Acta* **1988**, *150*, 25.
(4) Endo, A.; Zhang, W.; Shimizu, K.; Satô, G. P. Presented at the The Annual Meeting of the Chemical Society of Japan, 1997, Saint Paul University, Tokyo, Japan.
(5) Matsumoto, K.; Matsumoto, T.; Kawano, M.; Ohnuki, H.; Sichi, Y.; Nishide, T.; Sato, T. J. *J. Am. Chem. Soc.* **1996**, *118*, 3597 and references therein.
(6) Yamazaki, S.; Ama, T.; Hojo, M.; Ueno, T. *Bull. Chem. Soc. Jpn.* **1989**, *62*, 4036.

S0020-1669(97)01240-8 CCC: $15.00
Published on Web 09/15/1998

Table 1. Crystal Data and Structure Refinement for $2\cdot CH_3CN$ and $2'\cdot 1.25CHCl_3$

	2	**2′**
empirical formula	$Ru_2C_{27}H_{37}O_{10}SN$	$Ru_4C_{52.5}H_{70.5}O_{20}S_2Cl_{7.5}$
fw	769.79	1755.92
cryst syst	monoclinic	monoclinic
space group	$P2_1/n$ (No. 14)	$P2_1/n$ (No. 14)
unit cell dimens		
a/Å	11.388(3)	16.281(3)
b/Å	23.390(3)	21.195(2)
c/Å	11.978(3)	21.465(3)
β/deg	93.06(2)	105.75(1)
Z	4	4
V/Å^3 3185(1)	7128(4)	
ρ(calcd)/g cm^{-3}	1.605	1.636
μ/cm^{-1}	10.7	12.3
λ/Å	0.710 69	0.710 69
T/°C	20	20
R[a]	0.056	0.049
R_w[b]	0.042	0.042

[a] $R = \Sigma||F_o| - |F_c||/\Sigma|F_o|$. [b] $R_w = [\Sigma w(|F_o| - |F_c|)^2/\Sigma w|F_o|^2]^{1/2}$.

Experimental Section

Physical Measurements. ^{1}H and ^{13}C NMR spectra were recorded in $CDCl_3$ with the use of a JEOL GX-270 spectrophotometer. UV−visible spectra were recorded on a Hitachi Model U-3210 spectrometer. Electron impact ionization (EI) and fast atom bombardment (FAB) mass spectrometry (MS) experiments were carried out by using a JEOL JMS-D300 or JMS-SX102A. XPS were obtained at room temperature in an SSX-100 series (S.S.I.Co Lid) photoelectron spectrometer, employing an AEI monochromatized Al Kα X-ray source (1486.7 eV). The C 1s binding energy (284.6 eV) of the γ-carbon of acac$^-$ present in the ruthenium complexes was used for the calibration of the binding energy. The reproducibility of the measurements was ±0.1 eV. The instrument is fitted with insertion locks, which allow samples to go from atmospheric pressure to 10^{-6} Torr and ultimately to 10^{-9} Torr without bakeout. A 10 mg amount of the sample prepared in the form of pellet a was first brought to 10^{-6} Torr and kept overnight before being brought to 10^{-9} Torr for measurement. All of the sample preparations and mountings were carried out in an Ar-filled glovebox directly connected to the sample chamber of the spectrometer. Magnetic moments were obtained for the solid samples by the Faraday method, using Hg[Co(SCN)$_4$] as the calibration standard at 20 °C ($\chi_g = 16.44 \times 10^{-6}$ cm^3 g^{-1}, $\partial\chi/\partial T = -0.05 \times 10^{-6}$ cm^3 g^{-1}). In the calculation of the magnetic moment, the values of -52×10^{-6} cm^3 mol^{-1} for acac$^-$ and -59×10^{-6} cm^3 mol^{-1} for topd ligand were used as diamagnetic parameters. EPR measurements were carried out by using a JEOL JES-RE3X in EtOH.

X-ray Crystallography. Crystal data and structure determination parameters are given in Table 1. Single crystals of **2** were grown by the vapor diffusion of diethyl ether into a saturated solution of **2** in acetonitrile. Single crystals of **2′** were grown using a simple solvent diffusion method by the addition of hexane to a saturated solution of **2′** in chloroform. Single-crystal data collections for **2** and **2′** were performed at 293 K with a Rigaku AFCSS diffractometer using graphite-monochromated Mo Kα ($\lambda = 0.710\ 69$ Å) radiation. The unit cell parameters were calculated by least-squares refinement of 25 well-centered reflections in the range $20.38° < 2\theta < 23.1°$ for **2** and $20.47° < 2\theta < 23.88°$ for **2′**. The data were collected by the $\omega/2\theta$ scan mode. ω scans of several intense reflections made prior to data collection had an average width at half-height of 0.16° with a takeoff angle of 60°. Scans of $(1.42 + 0.30 \tan\theta)°$ were made at a speed of 6.0°/min (in ω). The weak reflections ($I < 10.0\sigma(I)$) were scanned (maximum of three scans) and the counts were accumulated to ensure good counting statistics. Stationary background counts were recorded on each side of the reflection. The ratio of peak counting time to background counting time was 2:1. The diameter of the incident beam collimator was 1.0 mm, the crystal to detector distance was 258 mm, and the detector aperture measured 9.0 mm × 13.0 mm (horizontal × vertical). The data were corrected for Lorentz and polarization effects. An empirical absorption correction using the program the DIRDIF[7] was applied. The structure was solved by heavy-atom Patterson methods and expanded using Fourier techniques with DIRDIF program.[7] The non-hydrogen atoms were refined anisotropically. Hydrogen atoms were included but not refined. The final cycle of full-matrix least-squares refinement was based on 2386 reflections ($I > 3.00\sigma(I)$) and 370 variable parameters and converged (largest parameter was 0.29 times its esd) with unweighted agreement factors of $R = \sum||F_o| - |F_c||/\sum|F_o| = 0.056$ and $R_w = [\sum w(|F_o| - |F_c|)^2/\sum w|F_o|^2]^{1/2} = 0.042$ for **2** and $R = 0.049$ and $R_w = 0.042$ for **2′** based on 8034 observed reflections and 793 variable parameters. The standard deviation of an observation of unit weight was 1.75 for **2** and 2.24 for **2′**. The weighting scheme was based on counting statistics and included a factor ($p = 0.012$ for **2** and $p = 0.004$ for **2′**) to downweight the intense reflections. Plots of $\sum w(|F_o| - |F_c|)^2$ versus $|F_o|$, reflection order in data collection, $\sin(\theta/\lambda)$, and various classes of indices showed no unusual trends. The maximum and minimum peaks on the final difference Fourier map corresponded to 0.63 and − 0.54 e$^-$/Å^3, respectively, for **2** and 1.14 and −0.91 e$^-$/Å^3, respectively, for **2′**. Neutral atom factors were taken from Cromer and Weber.[8] Anomalous dispersion effects were included in $F_{calc.}$[9] The values for $\Delta f'$ and $\Delta f''$ were those of Creagh and McAuley.[10] The values for the mass attenuation coefficients are those of Creagh and Hubbel.[11] All of the calculations were performed using the teXsan[12] crystallographic software of Molecular Structure Corporation.

Voltammetric Analysis. The voltammetric equipment used here has been described previously.[13] A suitable optically transparent thin-layer electrochemical electrode (OTTLE) cell[14] was fabricated in this laboratory and used for in situ measurement of the visible absorption spectra during electrolysis. The effective light path length and volume of the OTTLE were about 0.3 mm and 60 mm^3, respectively. Spectral measurement for OTTLE was performed using a spectro-multichannel photodetector (Photal MCPD-1000) with a personal computer (NEC PC-8801VX) and a plotter (Photal MC-920). All of the potentials were measured against an aqueous Ag|AgCl (3 mol dm^{-3} NaCl solution) reference electrode from Bioanalytical Systems (BAS). The reference electrode was connected to the test solution through a salt bridge with a Vycor plug filled with the background solution. The potential of the reference electrode was determined against the half-wave potential of the Fc/Fc^+ couple as an internal standard. The average potential of the reference electrode at 25 °C was -0.47 ± 0.01 V against the half-wave potential of the Fc/Fc^+ couple. A platinum disk of diameter 1.6 mm from BAS was used as the test electrode for cyclic and normal pulse voltammetric experiments except in cyclic voltammetry with high-potential scan. In this case, an ultramicro platinum disk electrode from BAS (10 μm diameter) was used. A platinum rotating-disk electrode of 2.0 mm diameter embedded in Teflon was used for the hydrodynamic voltammetry. A spiral platinum wire was used as the auxiliary electrode.

The reversible half-wave potentials $E_{1/2}$ were determined from the normal pulse or the hydrodynamic voltammograms by means of the conventional logarithmic plot method in the Nernstian case. In quasi-reversible cases, $E_{1/2}$ was approximated by $(E_{pa} + E_{pc})/2$, where E_{pa} and

(7) Beurskens, P. T.; Admiral, G.; Buerskens, G.; Bosman, W. P.; Garcia-Grenda, S.; Gould, R. O.; Smith, J. M. M.; Smykalla, C. The DIRDIF program system; Technical Report; Crystallography Laboratory, University of Nijmegen: Nijmegen, The Netherlands, 1992.
(8) Cromer, D. T.; Weber, J. T. *International Tables for X-ray Crystallography*; The Kynoch Press: Birmingham, England, 1994; Vol. IV, Table 2.2A.
(9) Ibers, J.A.; Hamilton, W.C. *Acta Crystallogr.* **1964**, 17, 781.
(10) Creagh, D. C.; McAuley, W. J. In *International Tables for X-ray Crystallography*; (Wilson, A. J. C., Ed.; Kluwer Academic Publishers: Boston, 1992; Vol. C, pp 219−222.
(11) Creagh, D. C.; Hubbel, J. H. In *International Tables for X-ray Crystallography*; (Wilson, A. J. C., Ed.; Kluwer Academic Publishers: Boston, 1992; Vol. C, pp 200−206.
(12) *teXsan Crystal Structure Analysis Package;* Molecular Structure Corporation: 1985 and 1992.
(13) Ushijima, H.; Kajitani, M.; Shimizu, K.; Satô,G. P.; Akiyama, T.; Sugimori, A. *J. Electroanal Chem.* **1991**, *303*, 199.
(14) Endo A.; Mochida, I.; Shimizu, K.; Satô G. P. *Anal. Sci. Jpn.* **1989**, *62*, 709.

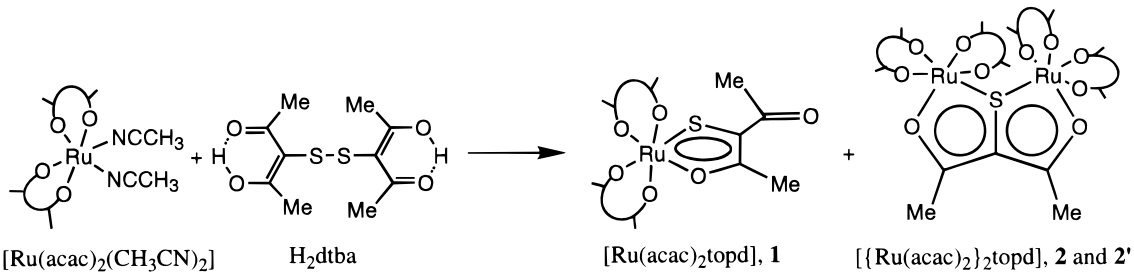

Figure 1. Reaction products of [Ru(acac)$_2$(CH$_3$CN)$_2$] and H$_2$dtba.

E_{pc} are the potentials of the anodic and cathodic peaks, respectively, of the cyclic voltammogram. In irreversible cases, $E_{1/2}$ was determined graphically from the normal pulse or the hydrodynamic voltammogram.

Materials. The purification of acetonitrile for electrochemical work was carried out as described previously.[15] Spectroscopic grade acetonitrile from Dojindo Laboratories was used for spectroscopic work. The supporting electrolyte was tetraethylammonium perchlorate (TEAP) (special polarographic grade) purchased from Nakarai Chemicals, Ltd. For synthetic experiments, commercially available reagent grade solvents and chemicals were used.

3,3′-Dithiobis(2,4-pentanedione) (H$_2$dtba). H$_2$dtba was synthesized from S_2Cl_2 and Hacac according to the literature method[16] and identified by EI MS, ^{1}H NMR, elemental analyses, and melting point.[17] [Ru^{II}(acac)$_2$(CH$_3$CN)$_2$] and [Ru^{II}(phpa)$_2$(CH$_3$CN)$_2$] were prepared by methods reported earlier.[18]

[Ru(acac)$_2$(topd-*O*,*S*)] (1). H$_2$dtba (160 mg; 0.6 mmol) in acetone (50 cm^3) was added to 450 mg of [Ru(acac)$_2$(CH$_3$CN)$_2$] (1.18 mmol) in acetone (550 cm^3), and the mixture was stirred at 25 °C under an atmosphere of argon. The progress of the reaction was monitored by silica gel TLC. After 10 min of stirring, the color of the solution turned to purple from yellowish orange and the TLC showed the disappearance of the starting complex. Then the solvent was evaporated and the residue was chromatographed on a silica gel column. The purple fraction eluted using benzene−acetonitrile (4:1 v/v) was collected, and it was again chromatographed under the same conditions. The pure fraction was collected, and the solvent was evaporated. The residue was recrystallized from hexane, and the complex obtained was dried under vacuum. Yield: 105 mg (20.5% based on Ru). Anal**.** Calcd for RuC$_{15}$H$_{20}$O$_6$S: C, 41.86; H, 4.69; S, 7.44. Found: C, 41.82; H, 4.80; S, 7.36. FAB MS: m^+/z = 430 (M$^+$). IR: 1652 cm^{-1} (ν(CO)). ^{1}H NMR: δ = 2.06 (3H), 2.09 (3H), 2.43 (3H), 2.53 (3H) (β-methyl proton of acac$^-$), 3.01 (3H), 3.54 (3H) (methyl proton of topd), 5.50 (1H), 5.54 (1H) (methyne proton of acac$^-$). ^{13}C NMR: δ = 208.4 and 196.39 (topd-*C*O), 193.60, 191.57, 191.17,190.10 (acac-*C*O), 180.21 (topd-*C*S), 99.74, 99.33 (acac-*C*H), 25.64−29.68 (CH$_3$ of acac and topd). XPS: 284.60 eV (C 1s), 282.02 eV (Ru 3d$_{5/2}$) and 163.64 eV (S 2p). μ_{eff} = +0.40 μ_B.

[{Ru(acac)$_2$}$_2$(topd-*O*,*S*,*O*′)] (2, Racemic; 2′, Meso). H$_2$dtba (320 mg; 1.2 mmol) in acetone (50 cm^3) was added to 810 mg of [Ru(acac)$_2$(CH$_3$CN)$_2$] (2.12 mmol) in acetone (850 cm^3), and the mixture was heated under reflux for 2 h. Then the solvent was evaporated off. The residue was chromatographed on a silica gel column. When the mixture was eluted with benzene−acetonitrile (4:1 v/v), the third fraction gave a blue compound (**2**) and the fourth fraction gave a green compound (**2′**). They were collected separately and chromatographed again under the same conditions to obtain pure compounds. Then the solvent was evaporated off and the compounds were recrystallized from dichloromethane and dried under vacuum. Yield: **2** (racemic), 174 mg (22.7% based on Ru); **2′** (meso), 107 mg (14.0% based on Ru). **2** (racemic): FAB MS, m^+/z = 730 (M$^+$); ^{1}H NMR, δ = 2.01 (6H), 2.05 (12H), 2.40 (6H) (β-methyl proton of acac$^-$), 3.05 (6H) (methyl proton of topd), 5.34 (2H), 5.56 (2H) (methyne proton of acac$^-$); XPS, 284.44 (C 1s), 281.15 (Ru 3d$_{5/2}$), and 163.71 eV (S 2p); μ_{eff} = +0.77 μ_B. Anal. Calcd for Ru$_2$C$_{25}$H$_{34}$O$_{10}$S: C.41.10; H, 4.69; S, 4.38. Found: C, 41.13; H, 4.63; S, 4.60. **2′** (meso): FAB MS, m^+/z = 730 (M$^+$); ^{1}H NMR, δ = 1.95 (6H), 2.00 (6H), 2.18 (6H), 2.42 (6H) (β-methyl proton of acac), 3.08 (6H) (methyl proton of topd), 5.25 (2H), 5.69 (2H) (methyne proton of acac); ^{13}C NMR, δ = 201.51 (topd-*C*O), 191.14, 189.68, 188.05, 186.92 (acac-*C*O), 165.15 (topd-*C*S), 99.32, 99.00 (acac-*C*H), 25.61−27.48 (*C*H$_3$ of acac and topd); XPS, 284.5 (C 1s), 281.17 (Ru 3d$_{5/2}$), and 163.43 eV (S 2p); μ_{eff} = 0 μ_B. Anal. Calcd for Ru$_2$C$_{25}$H$_{34}$O$_{10}$S: C, 41.10; H, 4.69; S, 4.38. Found: C, 41.31; H, 4.68; S, 4.42.

[{Ru(phpa)$_2$}$_2$(topd-*O*,*S*,*O*′)] (3, Racemic; 3′, Meso). The complex used in this reaction, [Ru(phpa)$_2$(CH$_3$CN)$_2$], is unstable in air. Hence, this complex after its preparation from 860 mg of [Ru(phpa)$_3$] (0.5 mmol) is used as such. H$_2$dtba (210 mg; 0.08 mmol) in acetone (50 cm^3) was added to the above acetone solution of [Ru(phpa)$_2$(CH$_3$CN)$_2$] (550 cm^3), and the mixture was heated under reflux for 30 min under an atmosphere of argon. The color of the solution turned to purple from yellowish orange. The solvent was evaporated off. The residue obtained was chromatogaphed on a silica gel column, and a green fraction was collected by eluting with benzene-acetonitrile (10:1 v/v). The solvent was evaporated off, and the residue obtained was again chromatographed on a silica gel column under the same conditions as before. There were two green fractions: the fifth one contained **3**, and the sixth fraction contained **3′**. The solvent was evaporated off, and the complexes **3** and **3′** were dried under vacuum. Yield: **3** (racemic), 30 mg (5.6% based on [Ru(phpa)$_3$]); **3′**(meso), 20 mg (3.8% based on [Ru(phpa)$_3$]). **3** (racemic): FAB MS, m^+/z = 1066 (M$^+$); ^{1}H NMR, δ = 0.94 (18H), 1.01 (18H), 1.04 (18H), 1.27 (18H) (*tert*-butyl proton of phpa), 3.00 (6H) (methyl proton of topd), 5.49 (2H), 5.80 (2H) (methyne proton of phpa). Anal. Calcd for Ru$_2$C$_{49}$H$_{82}$O$_{10}$S: C, 55.24; H, 7.76; S, 3.01. Found: C, 55.58; H, 7.79; S, 2.84. **3′** (meso): FAB MS, m^+/z = 1066 (M$^+$); ^{1}H NMR, δ = 0.98 (18H), 1.03 (18H), 1.07 (18H), 1.22 (18H) (*tert*-butyl proton of phpa), 3.00 (6H) (methyl proton of topd), 5.38 (2H), 5.83 (2H) (methyne proton of phpa). Anal. Calcd for Ru$_2$C$_{49}$H$_{82}$O$_{10}$S: C, 55.24; H, 7.76; S, 3.01. Found: C, 55.55; H, 7.82; S, 3.09.

Results and Discussion

Synthesis. The reaction between [Ru(acac)$_2$(CH$_3$CN)$_2$] and H$_2$dtba in acetone at 25 °C under an argon atmosphere gave a mononuclear complex [Ru(acac)$_2$(topd-*O*,*S*)]. However, when the same reaction was carried out under refluxing conditions, two isomers of sulfur-bridged binuclear [{Ru(acac)$_2$}$_2$(topd-*O*,*S*,*O*′′)] were obtained (Figure 1). In addition to the above two complexes, an orange fraction was obtained in a very low yield, for which only a mass spectral analysis was possible. From the parent peak of m^+/z = 860 (M$^+$) and fragment peak of m^+/z = 561 (M − Ru(acac)$_2$), this could be identified as the dtba^{2-}-bridged binuclear ruthenium(III) complex [(acac)$_2$Ru(μ-dtba)-Ru(acac)$_2$]. In the case of the sulfur-bridged binuclear complex, three kinds of isomers are possible: they are $\Delta-\Delta$, $\Lambda-\Lambda$ and $\Delta-\Lambda$. We could isolate only two isomers, i.e., **2** consisting of racemic form ($\Delta-\Delta$, $\Lambda-\Lambda$) and **2′** consisting of the meso form

(15) Endo, A.; Watanabe, M.; Hayashi, S.; Shimizu, K.; Satô G. P. *Bull. Chem. Soc. Jpn.* **1978**, *51*, 800.
(16) Magnani, F.; Angeri, A. *Gazz. Chim. Ital.* **1894**, *24-I*, 342.
(17) EI MS: m^+/z = 262. ^{1}H NMR: δ = 2.38(12H, β-methyl), 17.00 (2H, enol proton). Elemental anal. Found: C, 45.68; H, 5.19; S, 24.14. Calcd: C, 45.80; H, 5.34; S, 24.42.
(18) Kasahara, Y.; Hoshino, Y.; Shimizu., K.; Satô, G. P. *Chem. Lett.* **1990**, 381.

Scheme 1. Formation of the Mononuclear and the Binuclear Complexes of Ruthenium

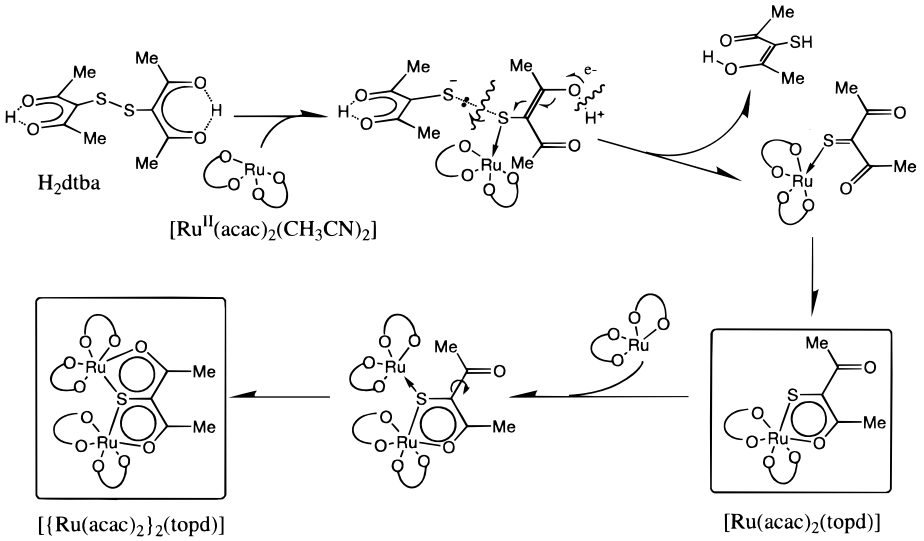

($\Delta-\Lambda$). X-ray single-crystal analysis confirmed the formulation of **2** and **2′** (to be described later). When the trivalent ruthenium complex $[Ru^{III}(acac)_2(CH_3CN)_2]^+$ was treated with H_2dtba even under refluxing conditions, no reaction seemed to take place; but a reaction between the mononuclear complex $[Ru^{II}(acac)_2$-(topd)] and $[Ru(acac)_2(CH_3CN)_2]$ yielded both **2** and **2′**. However, no reaction occurred between $[Ru^{II}(acac)_2(topd)]$ and $[Ru^{III}(acac)_2(CH_3CN)_2]^+$. These experimental observations indicate that the binuclear complex is formed by the addition of $\{Ru^{II}(acac)_2\}$ (formed by the dissociation of acetonitrile from $[Ru^{II}(acac)_2(CH_3CN)_2]$) to the mononuclear complex $[Ru^{II}$-$(acac)_2$(topd-*O*,*S*)] (Scheme 1). The first step in the reaction is the heterolytic cleavage of the S−S bond in H_2dtba, leading to the formation of thioxo β-diketone and thiol-β-diketone. The thioxo β-diketone binds the ruthenium of the $\{Ru(acac)_2\}$ unit through the sulfur atom and then through the oxygen atom, resulting in the formation of mononuclear complex **1**. Complex **1** adds another $\{Ru(acac)_2\}$ unit through the binding of the sulfur atom. Since there is no proton present at the γ-carbon atom, there is no possibility for enolization and, hence, the other oxygen atom of the carbonyl group should make a bond in such a way that complexes **2** and **2′** contain only neutral topd ligands.

A similar reaction of $[Ru(phpa)_2(CH_3CN)_2]$ with H_2dtba under refluxing conditions in acetone yielded two isomeric binuclear complexes of the type $[\{Ru^{II}(phpa)_2\}_2$(topd-*O*,*S*,*O*′)]. They have been identified as racemic (**3**) and meso (**3′**) forms of the binuclear complex. Though X-ray single-crystal analyses could not be done for **3** and **3′**, the UV−visible spectra (to be discussed later) and the elution pattern in column chromatography do indicate that they are racemic and meso forms, respectively. Besides **3** and **3′**, many fractions were collected from the chromatography, but the yields of other products (one among them may be the mononuclear complex) were so low that they could not be characterized.

Spectroscopic Studies. In the IR spectrum of the mononuclear complex $[Ru^{II}(acac)_2$(topd-*O*,*S*)] (**1**) the free $\nu_{C=O}$ was observed at 1652 cm^{-1}. The bands observed at 1559 and 1516 cm^{-1} have been assigned to the coordinated C−O group of the β-diketone.[19] These observations clearly indicate that the bonding is through one sulfur and one oxygen atom, leaving one carbonyl group free. For the isomers of **2** and **2′**, the IR spectra look quite similar and the two bands appearing in the region from 1569 to 1517 cm^{-1} have been assigned to the coordinated C−O group. The IR spectra of **3** and **3′** also showed that the β-diketone binds the metal atom through both the oxygen atoms and a sulfur.

^{1}H NMR spectra of all of the complexes showed all of the protons associated with $acac^-$, $phpa^-$, and topd present in the complexes; they have been presented in the Experimental Section with assignments. In the proton NMR spectra of **1**, there were two signals, one at 5.50 ppm and the other at 5.54 ppm, corresponding to one proton (γ-H) each on the acac unit. There is no signal for a proton at the γ-position of the topd ligand. Hence, the topd ligand should be neutral (triketone form) with its sulfur and one of the oxygen atoms attached to the ruthenium. The binuclear complexes show the presence of protons at the γ-carbon atoms only on the $acac^-$ or $phpa^-$ ligands (two signals around 5.25−5.83 ppm corresponding to two protons each) and not on the topd ligand. Therefore, the topd ligand should be a neutral moiety (triketone form) in all of the binuclear complexes also.

The ^{13}C NMR spectral data of **1** and **2′** along with the assignments are given in the Experimental Section. One special feature of the spectra of these two complexes is the notable difference observed in the signals for topd-*C*O and topd-*C*S. There are two signals for topd-*C*O in **1** (208.42 and 196.39 ppm) whereas there is only one signal in **2′**, showing two different C═O groups in **1** and two equivalent C═O groups in **2′**. There is a difference of about 15 ppm in the topd-*C*S signals between **1** (180.21 ppm) and **2′** (165.15 ppm). This is due to the difference in bonding of the sulfur atom in these two complexes (nonbridging in **1** and bridging sulfur in **2′**).

The electronic spectra of all the new complexes have been taken in acetonitrile solution; they are presented in Figure 2. The absorption data along with the molar absorption coefficients are given in Table 2. Both the mononuclear and binuclear complexes showed three bands in the region from 632 to 269 nm. However, the band around 300 nm for the mononuclear complex is weak, and it is observed only as a shoulder. A difference of about 7 nm was observed for the 600 nm band for **2** and **2′** although the λ_{max} values for the other two bands were the same. It is to be pointed out here that there is no spectral difference between the isomers in the case of the binuclear complexes bridged by teraacetylethane $[\{Ru(acac)_2\}_2$-

(19) Nakamoto, K. *Infrared and Raman Spectra of Inorganic and Coordination Compounds*, 4th ed.; John Wiley & Sons: New York, 1986.

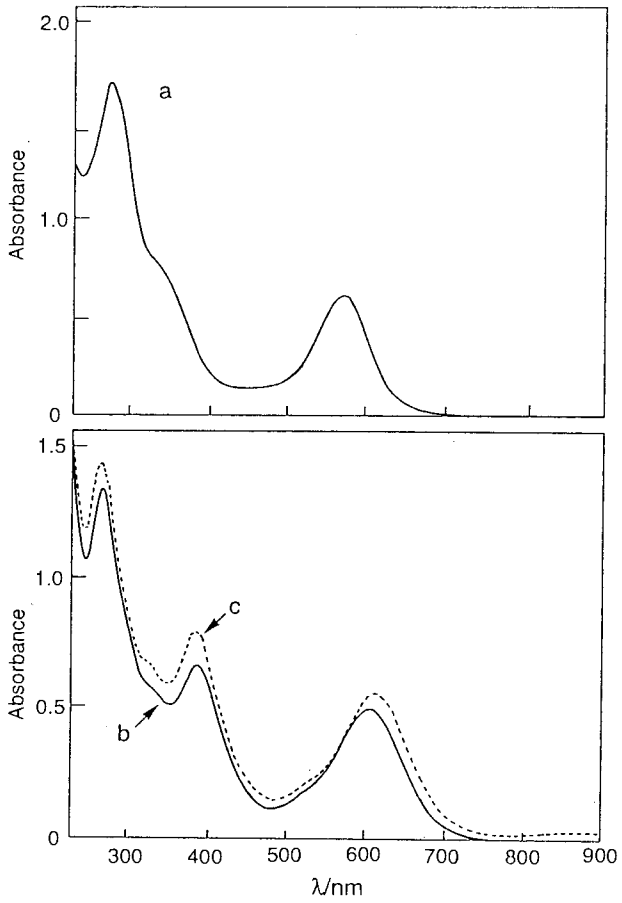

Figure 2. Electronic spectra of $[Ru(acac)_2(topd\text{-}O,S)]$ (a) and $[\{Ru(acac)_2\}_2(\mu\text{-topd-}O,S,O')]$[racemic (b) and meso (c)] taken in acetonitrile.

Table 2. Peak Wavelength (λ_{Max}) and Molar Absorption Coefficients (ϵ) of Mono- and Binuclear Complexes in Acetonitrile at 25 °C

complex	λ_{max}/nm	($\log(\epsilon/mol^{-1}dm^3\ cm^{-1})$)	
$[Ru(acac)_3]$	505 (3.16)	347 (3.87)	271 (4.18)
$[Ru(phpa)_3]$	496 (3.24)	368 (3.88)	279 (4.25)
$[Ru(acac)_2(topd)]$ (**1**)	569 (3.65)	332 (shoulder)	275 (4.09)
$[\{Ru(acac)_2\}_2(topd)]$			
2: racemic	607 (4.04)	388 (4.21)	269 (4.46)
2′: meso	614 (4.07)	388 (4.15)	269 (4.47)
$[\{Ru(phpa)_2\}_2(topd)]$			
3: racemic	614 (4.01)	397 (4.06)	274 (4.40)
3′: meso	623 (4.05)	396 (4.06)	272 (4.43)

$(tae)]^{20}$ (tae =1,1′,2,2′-tetraacetylethanate). The distances between the two $[Ru(acac)_{2]}$ units in **2** and **2′** are shorter than that present in $[\{Ru(acac)_2\}_2(tae)]$. Hence, the interactions of acac units present in **2** and **2′** might be responsible for the difference in λ_{max} for the 600 nm band. A very similar behavior is observed for **3** and **3′** also. Therefore, this electronic spectral behavior and the order of elution in the column chromatography do indicate that **3** and **3′** are racemic and meso forms, respectively.

In the case of the Ru^{III} complex $[Ru(acac)_3]$, an intense band is observed at 505 nm, whereas in the spectra of all of the new complexes, this band is observed around 600 nm, which is characteristic of either Ru^{II} or Ru^{IV}.[3] However, from the electronic spectral data alone, the oxidation state of ruthenium cannot be fixed.

In the electronic spectra of all of the binuclear complexes (**2**, **2′**, **3**, and **3′**) in acetonitrile solution, no absorption band corresponding to the metal−metal intervalence transfer (IT) was observed in the near-IR region (1000−2000 nm). Such electronic behavior together with the XPS, magnetic moments, and voltammetric characteristics (to be discussed later) is reasonably understood if the binuclear complexes are regarded as the mixed-valent complexes with valence-averaged ground states ($Ru^{II1/2} - Ru^{II1/2)}$, that is, class III in the Robin and Day classification.[21]

The XPS of the complexes **1**, **2**, and **2′** are shown in Figure 3 together with those of $[Ru^{II}(acac)_2(CH_3CN)_2]$ and $[Ru^{III}(acac)_3]$ as the reference compounds of Ru^{II} and Ru^{III}, respectively. The binding energies of Ru $3d_{5/2,}$ C 1s, and S 2p are given in the Experimental Section. The binding energy of Ru $3d_{3/2}$ is not discussed here because of the overlapping of the signal with that of C 1s. The Ru $3d_{5/2}$ binding energy of **1** (282.02 eV) is almost the same as that found for $[Ru^{III}(acac)_3]$. Such an energy value is an indication of the presence of Ru^{III}. The binding energies of Ru $3d_{5/2}$ for **2** and **2′** are 281.15 and 281.17 eV, which are intermediate between Ru^{III} and Ru^{II} found in $[Ru^{II}(acac)_2(CH_3CN)_2]$ (280.33 eV) and $[Ru^{III}(acac)_3]$ (282.20 eV). This means that the two binuclear complexes contain both Ru^{III} and Ru^{II}. If it is true, there must be two components for the Ru $3d_{5/2}$ binding energy corresponding to Ru^{III} and Ru^{II}; but the XPS of the binuclear complexes show only one peak and the peak profiles are similar to that of $[Ru^{III}(acac)_3]$. Therefore, the possibility of overlapping of the two components of Ru^{III} and Ru^{II} giving rise to a broad peak can be ruled out. Hence, there could be some kind of delocalization of electron between the two ruthenium atoms via the topd ligand. Alternatively, this can be described as a valence-averaged mixed-valent Ru^{III} and Ru^{II}. The same inference has been made from the voltammetric studies (to be discussed later). It is to be pointed out that in the case of a valence-averaged mixed-valent complex of $Ru^{III}-Ru^{II}$, almost the same value (281.0 eV) has been reported[5] for $[\{Ru(CH_3CN)_3(P(OMe)_3)_2\}_2(\mu\text{-}S_2)](PF_6)_3$. In the literature, the binding energies reported for Ru^{II} are 279.5−281.8 eV for $[Ru^{II}(NH_3)_5L]^{2+}$ (L represents various nitrogen donor ligands),[22] 279.9 eV for $[Ru^{II}(bipyridine)_2Cl_2]$,[23] and 279.6−280.8 eV for $[Ru^{II}(cp)(cp')]$ (cp′ is η^5-pentamethylcyclopentadienyl).[24] The binding energies for Ru^{III} are 281.8−281.9 eV for $[Ru^{III}(X\text{-}py)_2(DTBDiox)_2]ClO_4$ (X-py is halogenated pyridine, and DTBDiox is a derivative of 1,2-dioxolene),[25] 282.1−282.3 eV for $[Ru^{III}(NH_3)_5L]^{3+}$,[22] and 281.9 eV for $[Ru^{III}(bpy)_2Cl_2]Cl$.[23] A closer scrutiny of the above data and the data obtained for $[Ru^{III}(acac)_3]$ and $[Ru^{II}(acac)_2(CH_3CN)_2]$ and for our complexes shows the presence of Ru^{III} in **1** and Ru^{III} and Ru^{II} in **2** and **2′**. The binding energies of S 2p are almost the same as that reported[4] for disulfide S_2^{2-}. The binding energies of S 2p for the sulfur atoms in both mononuclear and binuclear complexes suggest that the sulfur atoms are present as S^-. In the case of the disulfide-bridged binuclear ruthenium(III) complexes[5] $[\{RuCl(P(OMe)_3)_2\}_2(\mu\text{-}Cl)_2(\mu\text{-}S_2)]$ and $[\{Ru(CH_3CN)(P(OMe)_3)_2\}_2(\mu\text{-}Cl)_2(\mu\text{-}S_2)]^{2+}$, the Ru^{III} $3d_{5/2}$ energies are 281.0 and 281.4 eV, whereas in the case of the oxo-bridged binuclear ruthenium complexes $[(bpy)_2ClRuORuCl(bpy)_2](PF_6)_2$

(20) Koiwa, T. M.S. Dissertation, Sophia University, Tokyo, Japan, 1990.

(21) Robin, M. B.; Day, P. *Adv. Inorg. Chem. Radiochem.* **1967**, *10*, 247.
(22) Sheperd, R. E.; Proctor, A.; Henderson, W. W.; Myser, T. K. *Inorg. Chem.* **1987**, *26*, 2440.
(23) Weaver, T. R.; Meyer, T. J.; Adeyemi, S. A..; Brown, G. M.; Eckberg, R. P.; Hatfield, W. E.; Johnson, E. C.; Murray, R. W.; Untereker, D. *J. Am. Chem. Soc.* **1975**, *97*, 3039.
(24) Gassman, P. G.; Winter, C. H. *J. Am. Chem. Soc.* **1988**, *110*, 6130.
(25) Auburn, P. R.; Dodsworth, E. S.; Haga, M.; Liu, W.; Nevin, W.A.; Lever, A. B. P. *Inorg. Chem.* **1991**, *30*, 3502.

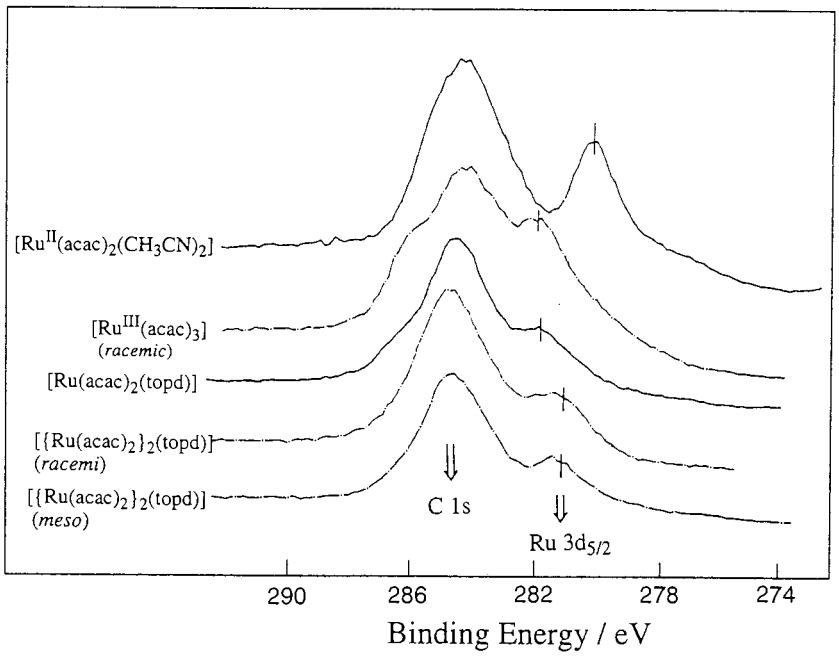

Figure 3. XPS of the new complexes and of reference complexes showing the binding energies of Ru $3d_{5/2}$ and C 1s.

and $[(bpy)_2(NO_2)RuORu(NO_2)(bpy)_2](ClO_4)_2$,[23] the Ru^{III} $3d_{5/2}$ energy is 280.5 eV.

Magnetic Moment and EPR. The magnetic moment values for **1** (0.17 μ_B) and **2′** (0 μ_B) indicate that they are diamagnetic, and hence we conclude the presence of Ru^{II} in these complexes. However, a slightly higher value of 0.77 μ_B is shown by complex **2**. This value is higher for Ru^{II} and lower for Ru^{III} when compared to the value of 0 μ_B for $[Ru^{II}(acac)_2(CH_3CN)_2]$ and a value of +1.95 μ_B for $[Ru^{III}(acac)_3]$. In order to check for the presence of Ru^{III} in **2,** the EPR spectra were run at room temperature and at liquid nitrogen temperature. No signal due to Ru^{III} could be observed, which would indicate the presence of Ru^{III} in complex **2**. Hence, the magnetic and EPR data for **1**, **2**, and **2′** show only the presence of Ru^{II} in the complexes; but XPS and voltammetric studies (to be discussed) do show a $Ru^{III}OS$ core for **1** and mixed-valent complexes with $Ru^{II}SRu^{III}$ cores in **2** and **2′**. A similar mixed-valent behavior has been observed in disulfide-bridged binuclear complexes with Ru^{II}-$SSRu^{III}$ cores and diamagnetism has been exhibited for Ru^{III} complexes of the types $[\{RuCl(TMP)_2\}_2(\mu\text{-}Cl)_2(\mu\text{-}S_2))]$ and $[\{RuCl(TMP)_2\}_2(\mu\text{-}Cl)_2(\mu\text{-}S_2))]^+$.

Structures of [{Ru(acac)$_2$}$_2$(topd)] (2, Racemic; 2′, Meso). The crystal of **2** is a racemic compound consisting of a pair of enantiomers Δ−Δ and Λ−Λ. The ORTEP plot of the Δ−Δ form is given in Figure 4. The value of $Z = 4$ in the $P2_1/n$ space group reveals that two molecules of Δ−Δ and two molecules of Λ−Λ coexist in one unit cell. This was confirmed by obtaining a Λ−Λ isomer by the operation of inversion through the center on a Δ−Δ isomer. The unit cell showing the coexistence of the two isomers is given in Figure 5. The bond distances, bond angles, and temperature factors for both of the isomers are the same. It has been found that there is one molecule of acetonitrile per molecule in the unit cell of complex **2**, and there is no bonding between acetonitrile and the ruthenium atom. The ORTEP plot of **2′** is given in Figure 6. In the unit cell of **2′**, there are two distinct types of molecules of **2′** (four molecules of each type in the unit cell along with 10 molecules of chloroform). It has been found that there is no interaction between the chloroform and the metal. Because of the disorder in the chloroform, the analysis could not be done precisely. Therefore, the two molecules of **2′** were treated separately. Though the C−S bond lengths in these two molecules differ, the geometry around the sulfur atom is the same. It is clear from the structures that the sulfur atom of the topd ligand bridges the two ruthenium atoms both in the racemic form, **2**, and in the meso form, **2′**. The major bond lengths and bond angles are listed in Tables 3 and 4.

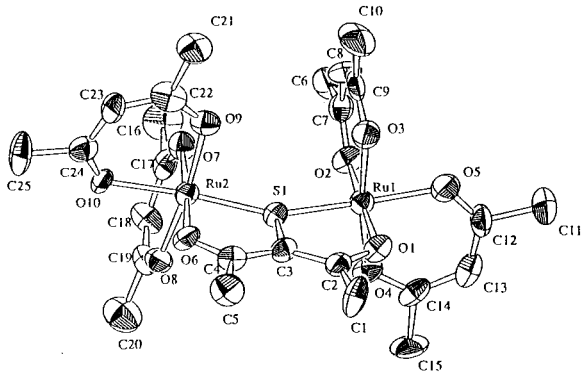

Figure 4. ORTEP plot of the complex **2** (Δ−Δ form) with the atomic labeling scheme.

There is no appreciable difference in bond lengths and bond angles found in **2** and **2′**. The bond lengths and bond angles of acetylacetone rings are almost the same as those reported for $[Ru(acac)_3]$.[26] The Ru−S bond length (2.168−2.178 Å) is slightly shorter than that found in other ruthenium(III) complexes: 2.195−2.290 Å in $[Ru(Ph\text{-}S)_3(CH_3CN)_2]$,[27] 2.208 Å in $[\{Ru(cp)(PMe_3)\}_2(\mu\text{-}S_2)]^{2+}$,[28] and 2.202−2.268 Å in a Ru^{III}−Ru^{II} dimer with a disulfide bridge.[5] A slightly longer distance (Ru−S) of 2.281 Å (average) for $[\{RuCl(PMe_3)_2\}_2(\mu\text{-}Cl)(\mu\text{-}N_2H_4)(\mu\text{-}S_2)]$[29] and 2.332 Å for $[\{Ru(CH_3CN)_3(PMe)_2\}(\mu\text{-}S_2)]$-

(26) Chao, G. K.; Sime, R. L.; Sime, R. J. *Acta Crystallogr.* **1973**, *B29*, 2845.
(27) Satsangee, S. P.; Hain, J. H.; Cooper, P. T.; Koch, S. A. *Inorg. Chem.* **1992**, *31*, 5160.
(28) Amarasekera, J.; Rauchfuss, T. B.; Wilson, S. R. *Inorg. Chem.*. **1987**, *26*, 3328.
(29) Hawano, M.; Matsumoto, K.; Hoshino, C. *Inorg. Chem.* **1992**, *31*, 5158.

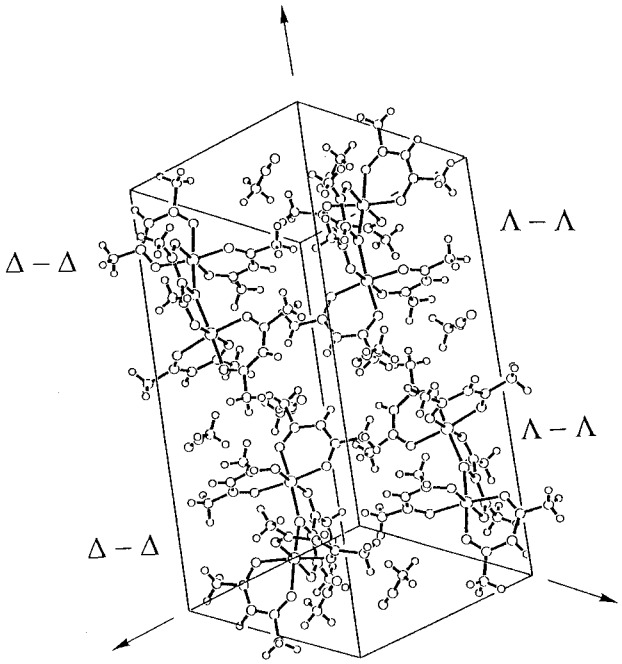

Figure 5. Unit cell of the complex **2** showing the coexistence of Δ−Δ and Λ−Λ forms.

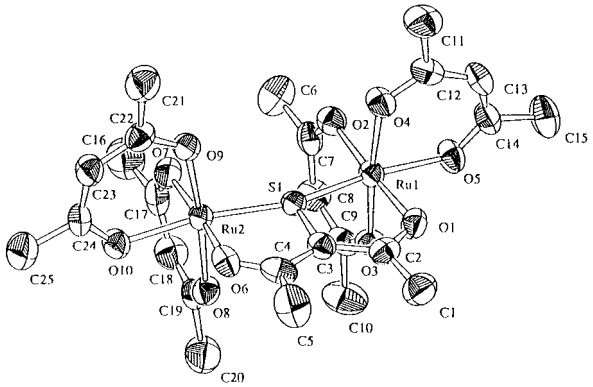

Figure 6. ORTEP plot of the complex **2′** (Δ−Λ, meso) with the atomic labeling scheme.

Table 3. Major Interatomic Distances (Å) for $2\cdot CH_3CN$ and $2'\cdot 1.25CHCl_3$

	2	**2′**		**2**	**2′**
Ru(1)−S(1)	2.168(4)	2.167(2)	Ru(2)−O(9)	2.035(8)	2.013(5)
Ru(2)−S(1)	2.178(4)	2.169(2)	Ru(2)−O(10)	2.051(8)	2.041(5)
Ru(1)−O(1)	2.052(8)	2.048(6)	S(2)−C(3)	1.73(1)	1.705(9)
Ru(2)−O(6)	2.047(8)	2.024(6)	O(1)−C(2)	1.26(1)	1.263(10)
Ru(1)−O(2)	2.035(7)	2.029(6)	O(6)−C(4)	1.26(1)	1.26(1)
Ru(1)−O(3)	2.009(8)	2.016(5)	C(2)−C(3)	1.39(2)	1.45(1)
Ru(1)- O(4)	2.025(8)	2.037(5)	C(3)−C(4)	1.44(2)	1.42(1)
Ru(1)- O(5)	2.016(9)	2.057(5)	C(1)−C(2)	1.58(2)	1.51(1)
Ru(2)−O(7)	2.050(8)	2.024(6)	C(4)−C(5)	1.48(2)	1.50(1)
Ru(2)- O(8)	2.018(8)	2.020(6)			

PF_6[5] have been reported. In complexes **2** and **2′**, the topd ligand forms an aromatic chelate ring; hence, the bond lengths and bond angles observed for topd are almost the same as that observed for the $acac^-$ ligand. Therefore, the aromaticity of the topd ring is responsible for the shorter Ru−S distance. Moreover, the bond length of C−S (1.73 Å) of the topd, which is intermediate between a single and a double bond, is also indicative of the aromaticity of the topd ring.

The dihedral angle between the planes containing Ru(1) − S(1) − O(1) and Ru(2) − S(1) − O(6) is 170.41°, showing the presence of the two ruthenium and the topd ligand in one plane in **2**. The dihedral angles of around 90° between any two β−diketone rings show an octahedral arrangement of ligands around the ruthenium atoms. A very similar observation has been made in the structure of **2′** also.

Table 4. Interatomic Angles (deg) for $2\cdot CH_3CN$ and $2'\cdot 1.25CHCl_3$

	2	**2′**
O(1) − Ru(1) − S(1)	82.4(3)	83.5(2)
O(6) − Ru(2) − S(1)	83.4(3)	83.0(2)
Ru(1) − S(1) − Ru(2)	153.1(2)	154.5(1)
O(2) − Ru(1) − O(3)	93.3(3)	93.7(2)
O(4) − Ru(1) − O(5)	90.8(4)	89.9(2)
O(1) − Ru(1) − O(2)	177.3(3)	177.1(2)
O(3) − Ru(1) − O(4)	173.0(4)	173.9(2)
O(5) − Ru(1) − S(1)	169.7(3)	172.0(2)
O(7) − Ru(2) − O(8)	92.9(3)	92.8(3)
O(9) − Ru(2) − O(10)	90.5(3)	90.2(2)
O(6) − Ru(2) − O(7)	175.6(3)	174.9(2)
O(8) − Ru(2) − O(9)	173.4(4)	173.9(2)
O(10) − Ru(2) − S(1)	170.8(3)	170.2(2)
Ru(1) − S(1) − C(3)	102.8(6)	102.8(3)
Ru(2) − S(1) − C(3)	101.8(6)	102.0(3)
Ru(1) − O(1) − C(2)	121.4(9)	119.5(8)
Ru(2) − O(6) − C(4)	120.4(6)	120.4(6)
S(2) − C(3) − C(2)	115(1)	114.3(7)
S(2) − C(3) − C(4)	113.4(10)	114.5(10)
O(1) − C(2) − C(3)	118(1)	119.4(8)
O(6) − C(4) − C(3)	120(1)	119.4(8)
C(2) − C(3) − C(4)	131(2)	131.2(8)

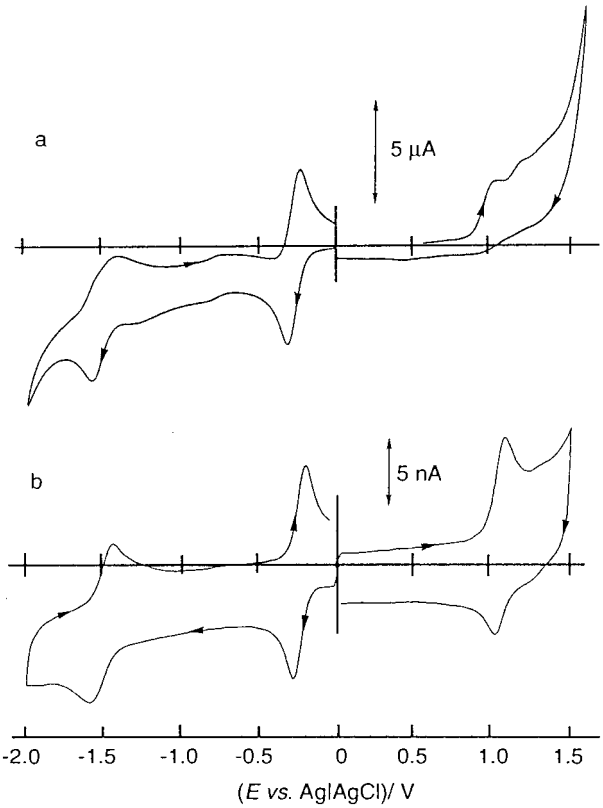

Figure 7. Cyclic voltammograms of the complex $[Ru(acac)_2(topd)]$ (**1**): (a) sweep rate = 100 mV s^{-1}, at platinum disk electrode (1.6 mm ∅) (b) sweep rate = 51.2 V s^{-1}, at ultramicro platinum disk electrode (10 μm ∅).

Voltammetric Behavior. A. $[Ru(acac)_2(topd)]$. A typical cyclic voltammogram of the mononuclear complex **1** showed one anodic peak together with subsequent small peaks, as shown in Figure 7a. Neither of the anodic peaks was accompanied by a corresponding reduction peak. At a high potential-sweep rate, however, a corresponding reduction peak appeared and the subsequent small peak disappeared, as shown in Figure 7b. The

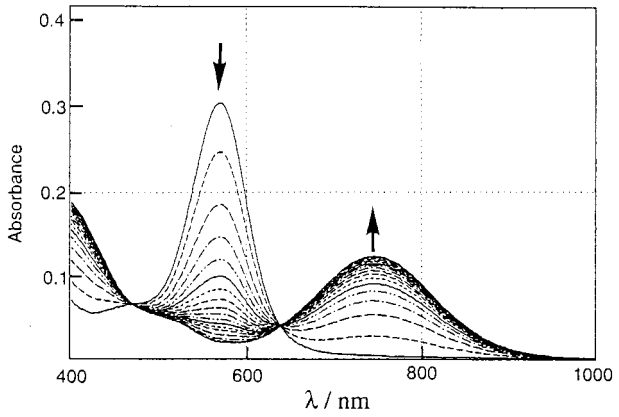

Figure 8. Electronic spectral changes during controlled-potential electrolysis using OTTLE for the complex $[Ru(acac)_2(topd)]$ (**1**).

Scheme 2. Electrochemical Reaction of the Mononuclear Complex **1**

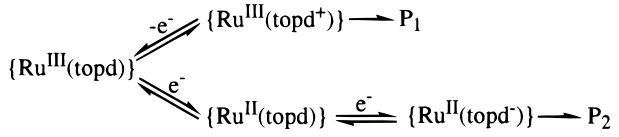

negative potential sweep showed two reduction peaks with accompanying coupled reoxidation peaks. Cyclic, normal, and hydrodynamic voltammetric analysis of the first reduction process revealed that this step was a Nernstian one-electron process ($E_{1/2} = -0.276$ V) without any subsequent chemical reaction. This is supported by (i) a value of $\Delta E_p = 68$ mV and $I_{pa}/I_{pc} \approx 1$ in its voltammogram; (ii) the plot of the limiting current versus $t^{-1/2}$ showing a straight line passing through the original point and its reciprocal slope being 27.8 mV in its normal pulse voltammogram; and (iii) the limiting currents being proportional to the square root of the angular rotation velocity in its hydrodynamic voltammetry. The second cathodic process was quasi-reversible in cyclic voltammetry. The charge numbers of electrode reactions for anodic and second cathodic processes were estimated to be unity by comparing with the peak height of the first cathodic step.

Figure 8 shows the spectral changes during the controlled potential electrolysis using OTTLE at -0.6 V for the reduction of **1**. In the one-electron reduction at -0.6 V (Figure 8), $\mathbf{1}^-$ was produced quantitatively without any side reactions at least up to 100 s. When the potential step was switched back to 0 V after complete reduction of **1**, the spectrum returned to the original shape quantitatively. This fact indicated that the one-electron-reduced species $[Ru(acac)_2(topd)]^-$ was fairly stable in the acetonitrile solution. Consequently, with the result of XPS and spectrophotometric experiments, we infer that the first reduction corresponds to Ru^{III} to Ru^{II} and both the second reduction and the oxidation correspond to the redox of the ligating topd ligand as represented in Scheme 2. The redox site in the topd ligand is probably the sulfur atom, since both products of the electrode reaction, $[Ru^{III}(acac)_2(topd^+)]$ and $[Ru^{II}(acac)_2(topd^-)]$, immediately give $\mathbf{P_1}$ and $\mathbf{P_2}$, respectively, which are not identified.

B. [{Ru(acac)$_2$}$_2$(topd)] (Racemic and Meso). The cyclic voltammogram of the binuclear complexes **2** and **2′** gave two reduction and two oxidation waves, as shown in Figure 9a,b. The voltammetric behavior of the racemic and meso forms is more or less the same. Both the first reduction and the first oxidation steps of **2** and **2′** were Nernstian and reversible one-electron processes. The second reduction process was quasi-reversible, and the second oxidation process was irreversible. Such voltammetric behavior was compared with that of the mononuclear complex **1**. A similar voltammetric behavior for the first oxidation and the first reduction processes in **2** and the first reduction process of **1** means that these oxidations and reductions are attributable to the metal-centered electron transfer reactions. Besides, the voltammetric behavior of the second oxidation and reduction of **2** and the second reduction of **1** are quite similar. These observations suggest that these electrode reactions correspond to the redox of the sulfur atom in the topd ligand. The voltammetric behavior of **3** and **3′** was the same as that of **2** and **2′**, except for a negative shift of the first oxidation and the first reduction potentials corresponding to the redox of the central metal (Figure 9c).

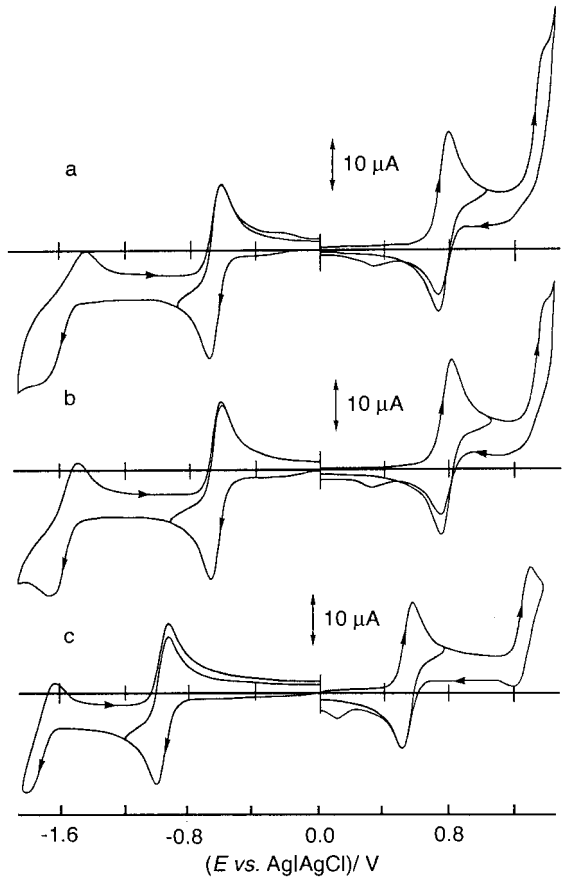

Figure 9. Cyclic voltammogram of the complexes [{Ru(acac)$_2$}$_2$(μ-topd-*O,S,O′*)], (a) for **2**, (b) for **2′**, and (c) for **3**, [{Ru(phpa)$_2$}$_2$(μ-topd-*O,S,O′*)].

The visible-spectral changes during the first reduction and the first oxidation of **2′** are shown in Figure 10. Both the reduced and oxidized forms of **2′** were fairly stable in acetonitrile solution. The feature of the visible spectral changes of the first reduction of **2′** is similar to that of **1**. This fact also supports that the first reduction should correspond to the reduction of Ru^{III} to Ru^{II}. Though it is very difficult to point out the site of first oxidation from the spectral changes alone, it is reasonable to believe that this is one of the ruthenium atoms in **2′**. Therefore, the binuclear complexes **2** and **2′** might be a mixed-valence complex of Ru^{III} and Ru^{II}. The electrode reactions of **2** and **2′** are represented in Scheme 3.

C. Redox Potential of the Mononuclear and Binuclear Complexes. The redox potentials of the complexes together with the comproportionation constants for the binuclear complexes are listed in Table 5. A positive shift of about 0.5 V in the reduction potential of Ru^{III} in **1** compared to that of [Ru-

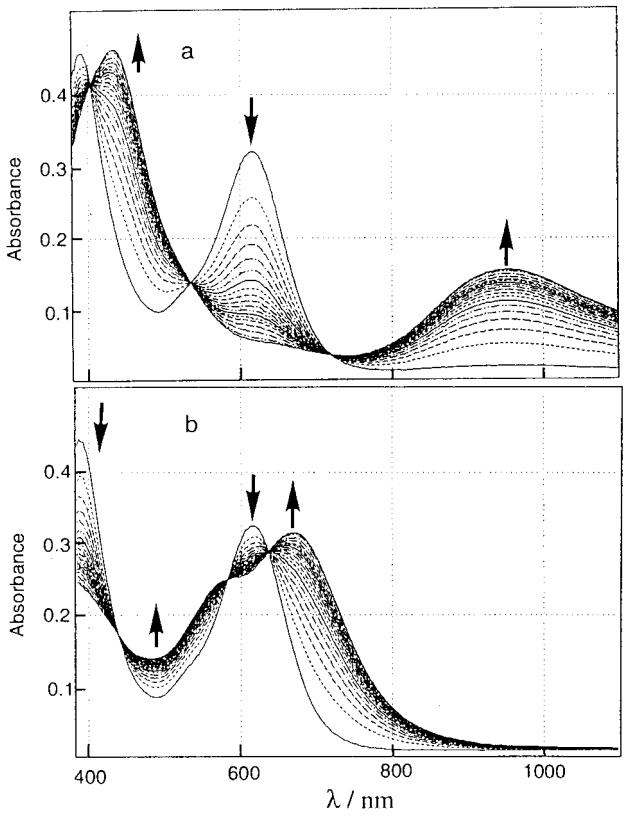

Figure 10. Electronic spectral changes during controlled-potential electrolysis using OTTLE for the complex [{Ru(acac)$_2$}$_2$(μ-topd-*O*,*S*,*O*′)] (**2**′): (a) reduction at −0.9 V; (b) oxidation at 1.0 V.

Scheme 3. Electrochemical Reactions of the Binuclear Complexes **2** and **2**′

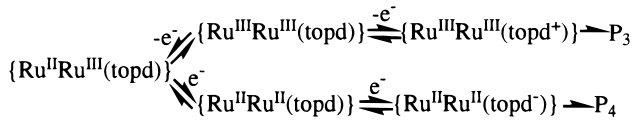

Table 5. Redox Potentials of the Mononuclear Complex 1, the Binuclear Complexes **2**, **2**′, **3**, and **3**′, and Related Complexes Together with the Comproportionation Constants, K_c, of the Binuclear Complexes

	redn		oxidn		
	$E_{1/2}(1)$ /V[a]	$E_{1/2}(2)$ /V	$E_{1/2}(1)$ /V[a]	$E_p(2)$ /V	log K_c
[Ru(acac)3]	-0.780		0.991		
[Ru(acac)$_2$(topd)] (**1**)	−0.275	−1.477	0.976		
[{Ru(acac)2}2(topd)]					
2: racemic	-0.665	−1.570	0.765	1.40	24.7
2′: meso	−0.629	−1.570	0.788	1.40	24.5
[Ru(phpa)2(acac)]	-0.960		0.790		
[{Ru(phpa)2}2(topd)]					
3: racemic	-0.971	−1.728	0.559	1.36	26.4
3′: meso	-0.975	−1.728	0.549	1.32	26.3

[a]The first oxidation and reduction potentials correspond to Ru^{II} to Ru^{III} and Ru^{III} to Ru^{II} in the complexes except [Ru(acac)$_3$] and [Ru(phpa)$_2$(acac)]. In the case of these complexes, the oxidation potential corresponds to Ru^{III} to Ru^{IV}.

(acac)$_3$] has been observed. Such a large positive shift suggests that a sulfur atom in the topd ligand accepts the electron from ruthenium more easily than the oxygen atom. The reduction potentials of Ru^{III} to Ru^{II} in **2** (−0.665 V) and **2**′ (−0.629 V) have been found to be shifted to about 0.4 V toward the negative side compared to that of **1** (−0.275 V). Such a large shift

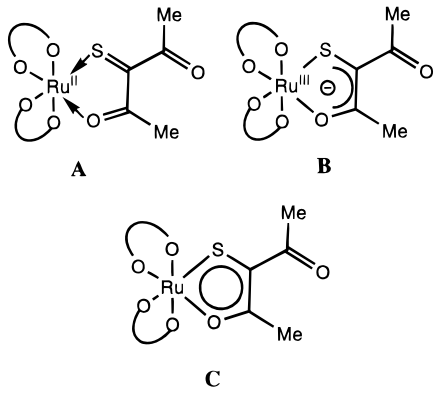

Figure 11. Two possible electronic structures (**A** and **B**) and the delocalization structure (**C**) of **1**.

toward the more negative side is due to the presence of Ru^{II} in the binuclear complexes in addition to Ru^{III} in them.

When acac$^-$ is substituted by phpa$^-$ in the binuclear complexes, the redox potentials of Ru^{III} to Ru^{II} and Ru^{II} to Ru^{III} shifted to the negative side by about 0.3 and 0.2 V, respectively. This is due to the increase in the electron-donating ability of phpa$^-$ as compared to acac$^-$. These potential shifts seem to coincide in magnitude with that of tris(β-diketonato)ruthenium complexes [Ru(acac)$_3$] and [Ru(phpa)$_2$(acac)].[30] The redox potentials of **2** and **2**′ are almost the same, and their reduction potentials shifted to 0.4 V toward the negative side compared to the mononuclear complex **1**. This is clearly an indication of the presence of at least one Ru^{II} in the binuclear complexes.

The equilibrium constant (K_c) for the comproportionation reaction in the binuclear systems is defined as

$$K_c = [M^{II}-M^{III}]^2/[M^{II}-M^{II}][M^{III}-M^{III}] = \exp[|E_{1/2}(1) - E_{1/2}(2)|F/RT]$$

where $E_{1/2}(1)$ and $E_{1/2}(2)$ are reversible half-wave potentials corresponding to ($Ru^{II}-Ru^{II}$)/($Ru^{III}-Ru^{II}$) and ($Ru^{III}-Ru^{II}$)/($Ru^{III}-Ru^{III}$), respectively. In our case, the K_c values for ($Ru^{II}-Ru^{III}$) of binuclear complexes have been calculated from the difference between $E_{1/2}(1)$ and $E_{1/2}(2)$. The K_c values (at 25 °C) of the binuclear complexes are presented in Table 5. Surprisingly, the values are extremely large compared to those of the binuclear complexes containing bridging bis(β-diketonate) where a direct bond is in between two acac$^-$ units (log K_c = 2.3−2.5) and where an ethynyl group is in between (K_c = 1.3−1.4)^2. It means that the binuclear complexes do not have distinct Ru^{II} and Ru^{III} in them whereas the valence averaged of the oxidation state is 2.5 on each ruthenium atom. In other words, there is extensive electron delocalization in the Ru−S−Ru core in all of the binuclear complexes.

Electronic Structure. The mononuclear complex **1** can have any one of the following structures depicted in Figure 11. ^{1}H NMR data correspond to structure **A** whereas the voltammetric and XPS data suggest structure **B**. If we consider Ru^{III} in the complex, the negative charge on the topd ligand can come from any one of the resonance structures in Figure 12. But the ^{1}H NMR spectra showed neither the proton of −OH nor the protons present at β or γ carbon atoms of the topd ligand. However, the magnetic measurements show that the mononuclear complex **1** is diamagnetic, indicating the absence of Ru^{III} in it. But, the voltammetric and XPS data not only strongly resemble those

(30) Haga, M.; Matsumura, T.; Shimizu, K.; Satô. G. P. *J. Chem. Soc., Dalton Trans.* **1989**, 371.

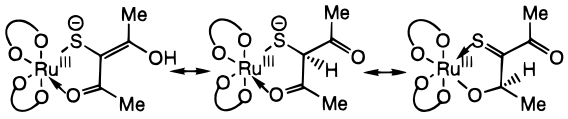

Figure 12. Possible electron distribution on the topd ligand in **1**.

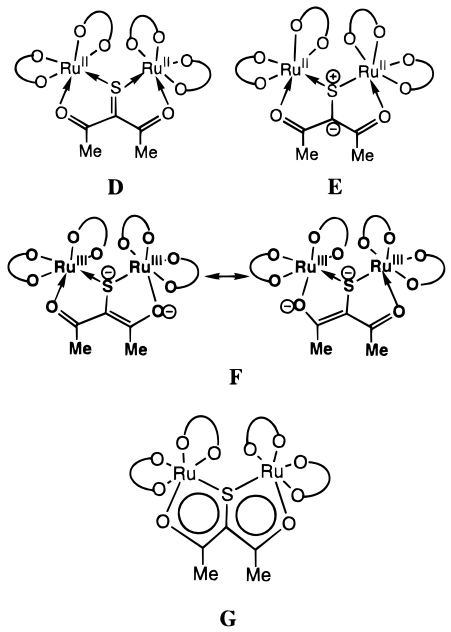

Figure 13. Possible electron distribution on the topd ligand with Ru(II) (**D** and **E**) and Ru(III) (**F**) and the delocalization structure (**G**) of **2** and **2′**.

of Ru^{III} but also are quite different from those of Ru^{II}. From the above discussions, it becomes very clear that complex **1** contains Ru^{III} and a negative charge on the topd ligand. Hence, on the basis of the spectroscopic and CV data, structure **C** could be proposed for **1**.

As for the structure of the racemic and meso forms of [{Ru(acac)$_2$}$_2$(topd)], the triketo (**D**) or ylide form (**E**) is suggested for the topd ligand (Figure 13); but their XPS show Ru $3d_{5/2}$ binding energy values that are intermediate between those of Ru^{III} and Ru^{II}. The voltammetric data also confirm at least one Ru^{III} to be present in **2** and **2′**. If one assumes the presence of Ru^{III}, then there are two possible resonance structures (**F**), both of which should show paramagnetism; but both **2** and **2′** show only diamagnetism. Moreover, the XPS data do not correspond to Ru^{III} but indicate a value intermediate between those of Ru^{III} and Ru^{II}. The same kind of observation has been made from the voltammetric data also. Hence, the above resonance structures do not fit quite well with the experimental data, although they certainly indicate the presence of at least one Ru^{III} and a negative charge on the topd ligand in all of the binuclear complexes. Therefore, one can think of a delocalization like the one shown in **G** (Figure 13) and a mixed-valent Ru^{III} and Ru^{II} in the complexes.

Conclusion

It is very reasonable to believe that **1** is a Ru^{II} complex with a neutral topd ligand as evidenced from its magnetic moment, EPR, and electronic spectral data, but the XPS and voltammetric data point to a Ru^{III} complex. Similarly, the magnetic and EPR data for the binuclear complexes indicate that they are Ru^{II} complexes, whereas their XPS and voltammetric data show that they are mixed-valent complexes containing a $(RuSRu)^{4-}$ core. Thus, in the case of the mixed-valent complexes with valence-averaged ($Ru^{II1/2}$—$Ru^{II1/2}$), the delocalized behavior of the electrons between ruthenium and the bridging ligand might be dependent on the magnitude of the time resolution of each technique.[31] The assignment of oxidation states becomes less meaningful if one assumes the binuclear complexes as covalent systems with $(RuSRu)^{4-}$ cores. Hence, all of the binuclear complexes (**2**, **2′**, **3**, and **3′**) are class III in the Robin and Day classification.[21]

Acknowledgment. We thankfully acknowledge Dr. Hirotaka Nagao for valuable discussions on the crystal structure determination. This work was partially supported by Grant-in-Aid for Scientific Research No. 8874083 from the Ministry of Education, Science and Culture, Japan.

Supporting Information Available: Details of the crystal data collection procedures for **2** and **2′**, anisotropic thermal parameters, interatomic distances, and bond angles (38 pages). Ordering information is given on any current masthead page.

IC971240R

(31) Creutz, C. *Prog. Inorg. Chem.* **1983**, *30*, 1.